Report **255**

A review of airborne gamma-ray spectrometric data-processing techniques
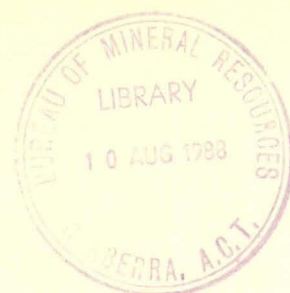
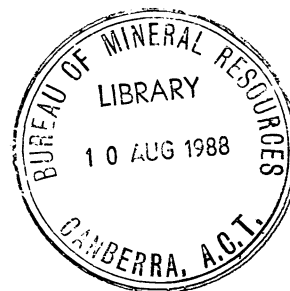B.R.S. Minty

Bureau of Mineral Resources, Geology and Geophysics

DEPARTMENT OF PRIMARY INDUSTRIES & ENERGY

BUREAU OF MINERAL RESOURCES, GEOLOGY AND GEOPHYSICS

Report No. 255

A REVIEW OF AIRBORNE GAMMA-RAY SPECTROMETRIC
DATA PROCESSING TECHNIQUES

by

B.R.S. Minty
(Division of Geophysics)

AUSTRALIAN GOVERNMENT PUBLISHING SERVICE
CANBERRA, 1988

CONTENTS

ABSTRACT

The development of interactive image-processing technology and its application to the presentation and interpretation of airborne gamma-ray spectrometer data has stimulated a new interest in the use of these data for regional geological mapping. The application demands sensitive detection equipment and sophisticated data processing procedures. This report, after describing the basic principles involved, reviews recent advances in airborne radiometric processing techniques. Several changes to the present system used by BMR and new avenues of research are recommended.

INTRODUCTION

In 1976 the Bureau of Mineral Resources (BMR) published a comprehensive review of procedures used in the acquisition, processing, and interpretation of airborne gamma-ray-spectrometer data (Wilkes, 1976). Since then there have been a number of significant advances. These include a trend towards the use of multichannel spectrometers to allow full spectrum analysis, the use of 'upward-looking' detectors to monitor atmospheric radiation, 'coincident detection' techniques to allow directional detection of radiation as well as photopeak spectra enhancement, and new techniques for the conversion of countrates to elemental abundances.

This report reviews recent developments in data processing and is timely especially for the following reason: whilst airborne gamma-ray spectrometry has always been viewed as a possible lithological mapping tool, it is only with the advent of interactive image-processing systems that this possibility has been realised (Richards & others, 1983). By assigning a primary colour to each of the radioelements (K, U, Th) and using current image processing technology including image enhancement, contrast stretching, principal-component analysis, etc., Richards & others (1983) report that the system '.... provides a means of interpreting airborne radiometric data much more quickly and exhaustively than any other methods currently available. It is overwhelmingly superior to contour maps, stacked profiles or multiplots for presenting and analysing this type of data. It is also cheaper'.

Very slight changes in radioelement abundances may be geologically significant, and this type of analysis, therefore, demands sensitive detection equipment and sophisticated data processing.

In general, observational or processing errors are magnified in subsequent processing stages, and, as Grasty (1975) points out, now that digital recording and automatic data processing have become an integral part of airborne surveys, there seems little point in carrying out approximations which can lead to considerable errors.

BASIC PRINCIPLES

Gamma spectrometry

The spontaneous disintegration of some atomic nuclei is accompanied by the emission of one or more alpha particles, beta particles, and gamma rays. Potassium, uranium, and thorium are the only elements with radioisotopes that are found in significant concentrations in the earth's crust. The decay of these radioisotopes and their daughters is sometimes accompanied by gamma-ray emissions whose energy is characteristic of their source. Thus, in gamma-ray spectrometry the measurement of gamma-ray photon energies allows the source of the radiation to be diagnosed.

^{40}K is the only radioactive isotope of potassium, and occurs as 0.012 percent of natural potassium. Eighty-nine percent of ^{40}K nuclei decay by electron emission (i.e. beta particle) to ^{40}Ca, while the remaining 11 percent decay by electron capture to ^{40}A, followed by the emission of a single gamma-ray photon with energy 1.46 MeV. ^{40}K occurs as a fixed proportion of K in the natural environment and the gamma-ray flux from ^{40}K is thus directly proportional to the total amount of K present.

Uranium occurs naturally as the radioisotopes ^{238}U and ^{235}U which give rise to decay series that terminate in the stable isotopes ^{206}Pb and ^{207}Pb respectively (Tables 1 and 2). ^{235}U forms only 0.72 percent of naturally occurring uranium, and because the gamma-energies in its decay series are concentrated in the 0.026-0.35 MeV range (i.e. outside the normal range of measurements), its effect is minimal. ^{234}U is naturally in secular equilibrium with ^{238}U and forms only 0.0057 percent of naturally occurring uranium. It is extremely unusual for the ratio ^{235}U/^{238}U to vary in nature.

Thorium occurs naturally as the radioisotope ^{232}Th which gives rise to a decay series that terminates in the stable isotope ^{208}Pb (Table 3).

Neither ^{238}U nor ^{232}Th emit gamma-rays, and we thus rely on the gamma-ray emissions from their radioactive daughter products to estimate their concentrations.

There are three principal processes by which gamma-rays interact with matter:

The photoelectric effect, in which all the energy of the photon is absorbed by the bound electron of an atom. This is the predominant absorption process at low energies.

Compton scattering, in which an incident photon loses part of its energy to an electron, and is 'scattered' at an angle to its original direction. This is the predominant process for moderate energies in most materials.

Pair production, in which the incident photon is completely absorbed, with the creation of an electron-positron pair in the electrostatic field of a nucleus and with a total energy equal to that of the original photon. This can occur at energies greater than 1.02 MeV and predominates at very high energies and particularly in materials of high atomic number.

Figure 1 illustrates the relationship between these processes, the gamma-ray energy of the incident photon, and the atomic number of the absorbing medium. From this it is clear that Compton scattering is the predominant process for the range of energies and absorbing media encountered in airborne gamma-ray
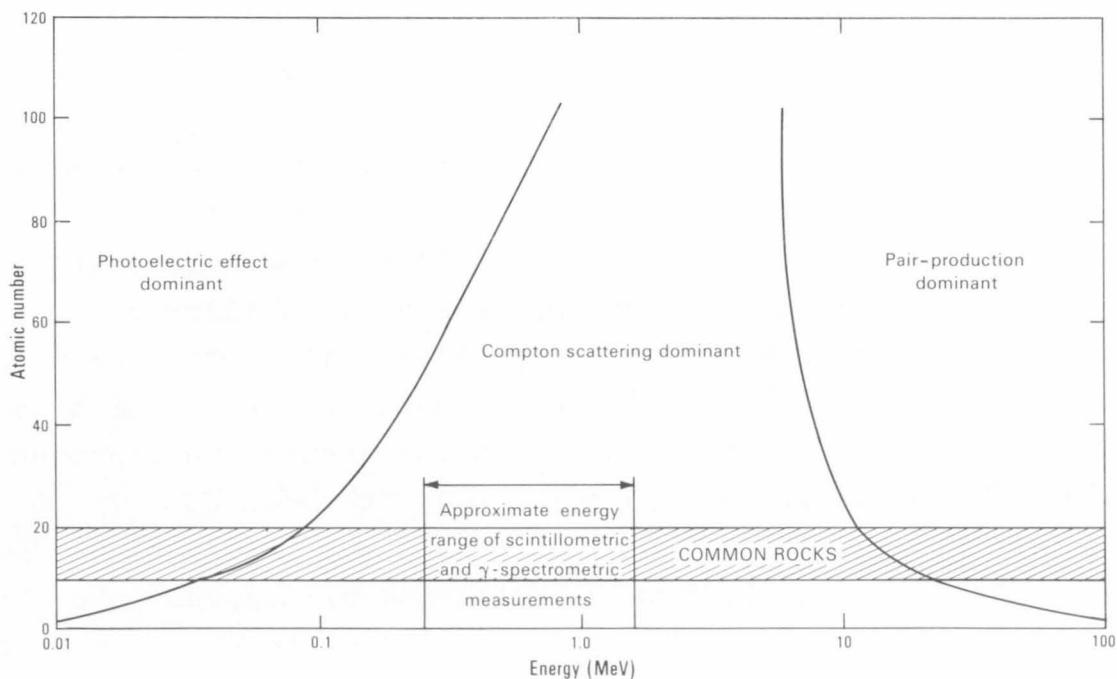
Fig. 1. Interaction of gamma-rays with matter
(after Fritzsche, 1982).

surveying. The gamma-ray photons lose energy through successive scattering events, until eventually the resulting low-energy photons are completely absorbed through the photoelectric effect.

The scattering and absorption of a gamma-ray in a thallium-activated sodium iodide crystal gives rise to a series of virtually simultaneous scintillations, the sum of which produce a pulse height in the detector proportional to the energy of the gamma-ray on entering the crystal. Thus NaI (Tl) detectors can discriminate between radiations from different nuclides, which is one of the reasons why they are the most commonly used scintillator in exploration today.

Disequilibrium

Disequilibrium in the uranium decay series is a serious source of error in gamma-ray spectrometer surveying.

When a radioisotope decays, producing an unstable daughter with a half-life shorter than that of the parent, a situation will eventually be reached where the daughter product is decaying as rapidly as it is being produced. If this is true for all the daughters in a decay series, then the series is said to be in secular equilibrium, and the total activity decreases at the same rate as that of the original parent.

Disequilibrium occurs when one or more decay products are completely or partially removed or added to the system (usually by geochemical processes), and it may take days, weeks or even millions of years to restore equilibrium, depending on the half-lives of the radioisotopes involved. There is no evidence to suggest that thorium ever occurs out of equilibrium in nature, and there are no disequilibrium problems with potassium since it only exhibits a single photo-peak. However, in the uranium decay series, disequilibrium is common in the natural environment and is mainly due to the following:

(a) ^{222}Rn (radon gas) is very mobile and can escape into the atmosphere from soils and rock fissures in response to the 'pumping' action of changing temperatures and pressures. Lovborg & others (1978) report that radiation output from Research Establishment Riso's uranium calibration pad near Roskilde, Denmark, is subject to a seasonal variation of ±20

percent. In warm, dry weather the concrete surface has a low
content of radon daughters because of excessive radon escape.
In cold, moist weather the situation is reversed. Similar
seasonal variations in uranium radiation output can be
expected in the natural environment.

(b) Both uranium and radium are soluble, and thus transportable.
In an oxidising environment, uranium is preferentially
leached relative to radium, and in a reducing environment
radium may be preferentially leached relative to uranium
(Bristow, 1983).

If ^{222}Rn escapes, the short-lived nuclides ^{214}Bi and
^{214}Pb which occur below ^{222}Rn in the uranium decay series and
are used to measure uranium concentration, will decay to
insignificant activities within hours. The replenishment to
equilibrium of ^{222}Rn will take about 38 days. Where there has
been preferential leaching of uranium relative to radium it will
take tens of thousands of years to re-establish equilibrium. In
this case the ^{214}Bi and ^{214}Pb concentrations will remain high
for many thousands of years even though the ^{238}U may have been
completely removed. This is due to the long half-lives of ^{234}U
and ^{230}Th which intervene between ^{238}U and ^{214}Bi/^{214}Pb in
the uranium decay series (Table 1).

Background radiation

Any radiation not originating from the ground is regarded as
'background', since it is of no geological significance and needs
to be removed from the observed data. There are four sources of
background radiation flux:

(a) Atmospheric ^{222}Rn and its daughter products - specifically
^{214}Bi and ^{214}Pb. This is the major contribution to the
background radiation, particularly in regard to the
estimation of uranium concentrations. Darnley & Grasty (1971)
report that on average for their three-channel system over 70
percent of photons detected in the uranium window arise from
radon daughter products occurring in the air. During warm
settled weather it is common for atmospheric ^{214}Bi and
^{214}Pb to be at a maximum close to the ground early in the

morning, and to decrease by 10-15 percent during the day as
atmospheric mixing occurs (Wilkes, 1976). Inversion layers
over topographic depressions and lakes often trap radon close
to the ground and under still-air conditions there can be
measurable differences in atmospheric radioactivity at sites
only a few kilometres apart (Darnley & Grasty, 1971). Larson
& Hoppel (1973) showed that radon levels generally decrease
with altitude but are still measurable at altitudes of up to
at least 4 km. Radioactive precipitation by thunderstorms
(Charbonneau & Darnley, 1970) can lead to apparent increases
of more than 2000 percent in uranium ground concentrations.
The tracks of heavy thunderstorms should thus be avoided in
airborne surveying until anomalous surface activity has had a
chance to decay (about 6 hours). A typical 'radon' spectrum
is given in Figure 2.
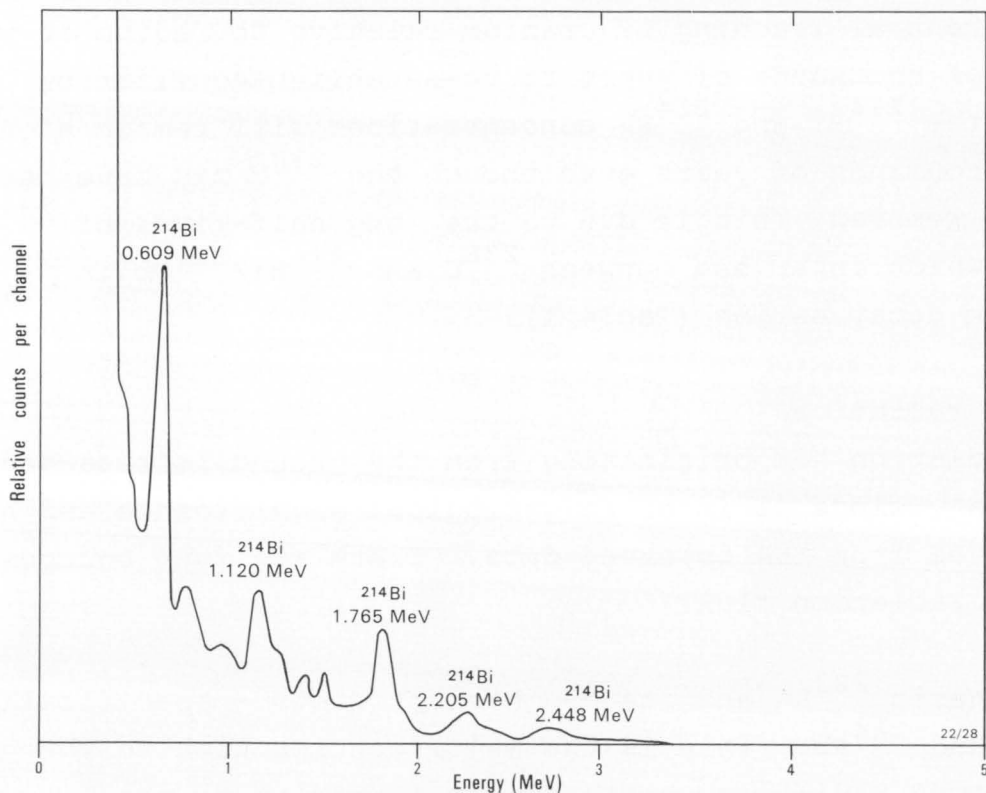
Fig. 2.   The radon daughter gamma energy spectrum
          (after Fritzsche, 1982).

(b) Primary cosmic radiation from outside our solar system and
from the sun reacts with atoms and molecules in the upper
atmosphere and generates complex secondary radiation. Below
about 12 km altitude this radiation has a constant energy
distribution, but it decreases in amplitude with decreasing
altitude. This radiation reacts with the air, aircraft, and
detector to produce the measured 'cosmic' spectrum which
decreases with increasing atmospheric pressure. Cosmic
radiation is also higher at high latitudes than at the
equator. The effect of cosmic ray interaction with rocks is
small (Gregory, 1960). A 'cosmic' spectrum is shown in
Figure 3. The single 0.511 MeV photopeak is due to
annihilation radiation originating from cosmic interactions
in the aircraft and detector.
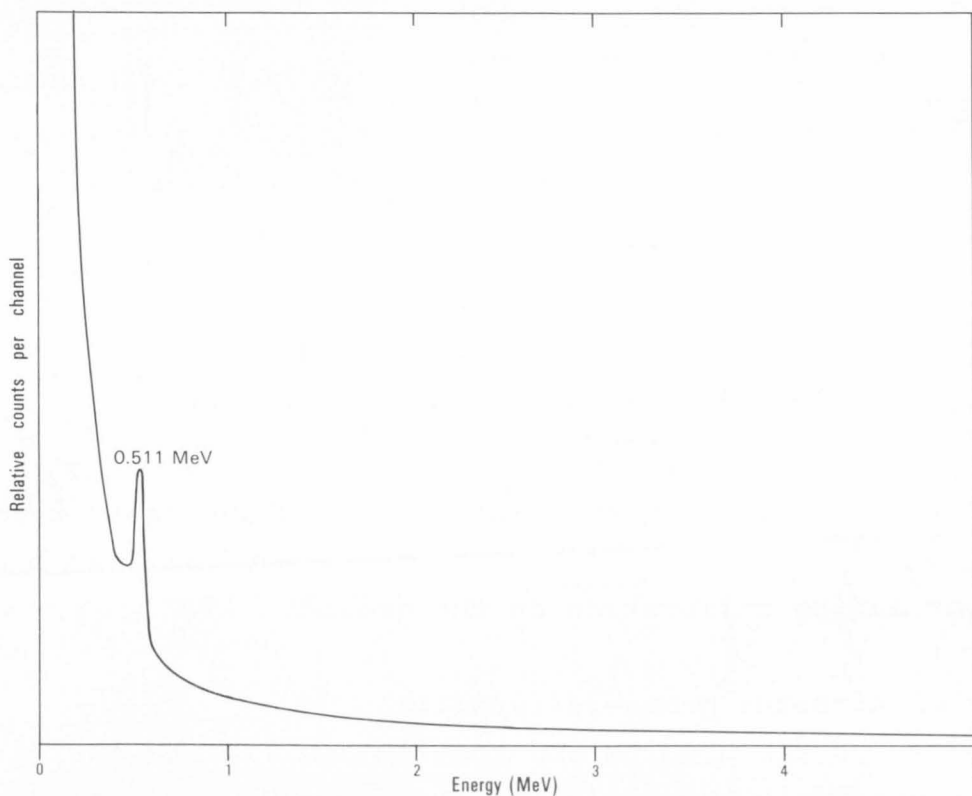
Fig. 3.   The cosmic gamma energy spectrum
(after Fritzsche, 1982).

(c) Radioactivity from the aircraft and its contents.
Radioactive contamination of the aircraft structure and
equipment as well as of the detector itself are the usual
contributors. However, radium used in luminous paints for

instrument dials and warning signs would also be a prime
source in older aircraft. An 'aircraft' spectrum is shown in
Figure 4.

(d) Atmospheric radiation due to fallout from nuclear explosions
(mainly ^{137}Cs). This contribution has decreased
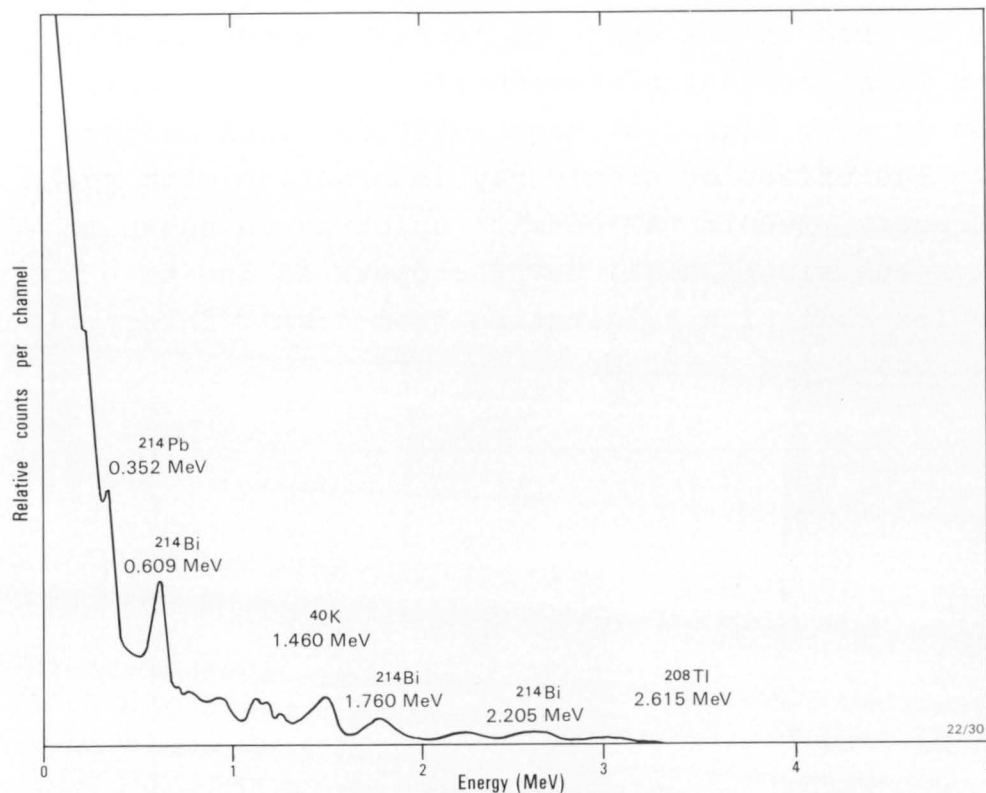
Fig. 4. The aircraft gamma energy spectrum
(after Fritzsche, 1982)

significantly since the ban on atmospheric nuclear tests over 15
years ago, but ^{137}Cs can still be detected - typically at high
altitudes or during calibration on the ground.

Properties of airborne gamma-ray spectra

Potassium and the uranium and thorium equilibrium series each
have a characteristic theoretical line spectrum. Figures 5 and 6
show the discreet gamma-ray energies associated with the
radioactive decay of uranium, thorium, and their decay products.
In practice it is impossible to record a line spectrum, since the
original energies of the photons are degraded by Compton
scattering in the source, in matter between the source and the
detector, and in the detector itself. This results in a measured

spectrum (or spectrogram) showing a continuous range of energies,
known as the Compton continuum, with well defined photopeaks
(Figures 7-9). In addition to the concentration of radioelements
in the source, the shape of the spectrum is thus a function of
the detector response, the source geometry, and the thickness of
attenuating material between the source and the detector. These
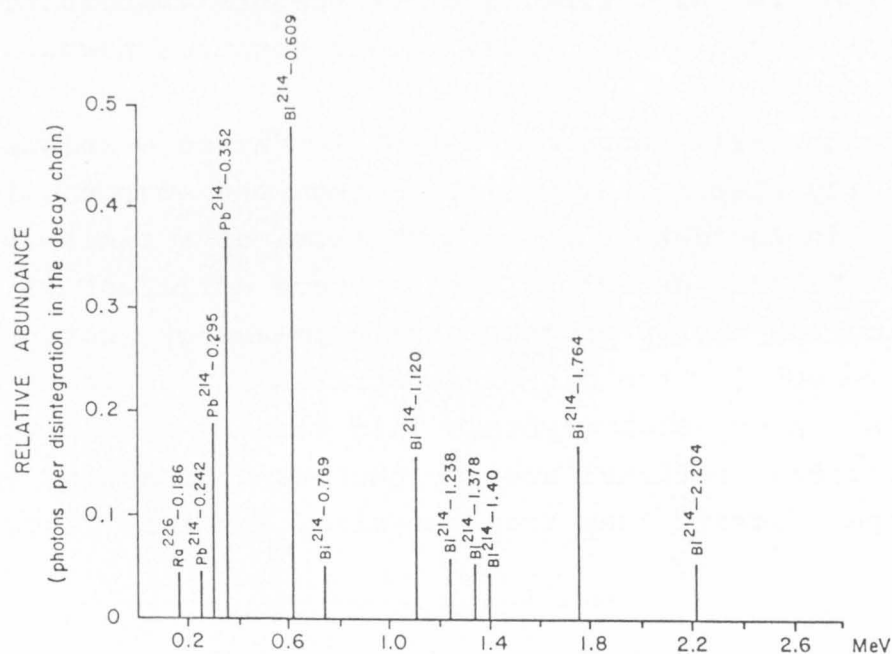
Fig. 5.   The uranium line spectrum (Reproduced from
          Bristow, 1983).
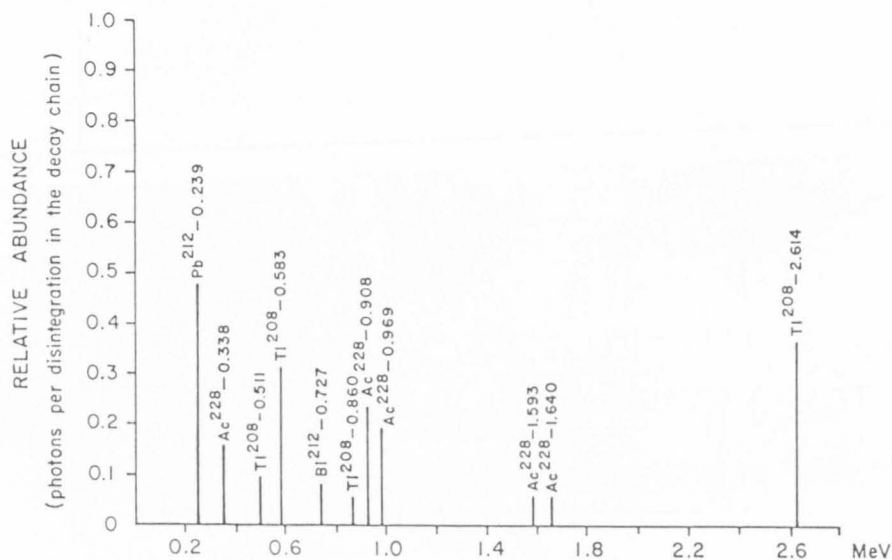
Fig. 6.   The thorium line spectrum (reproduced from
          Bristow, 1983).

are discussed below:

(a) **Detector response.** The detector modifies the spectrum
    considerably, and any analysis must incorporate the detector
    response. The main aspects are: (1) the detector efficiency
    as a function of energy, (2) directional sensitivity, (3)
    resolution, (4) dead time, and (5) factors contributing to
    the shape of the actual pulse height spectrum measured by
    spectrometers.

    Detector efficiency can be considered as a measure of the
    probability that a photon emitted from the source will
    interact in the detector, with the loss of a finite amount of
    energy. NaI(Tl) detectors are far more efficient at
    absorbing low-energy photons than high-energy photons. This
    is one reason for the higher countrates in the lower-energy
    channels. Also, slab crystals laid side by side present a
    greater cross-sectional area to photons approaching from
    below the aircraft than from the side, and this gives the
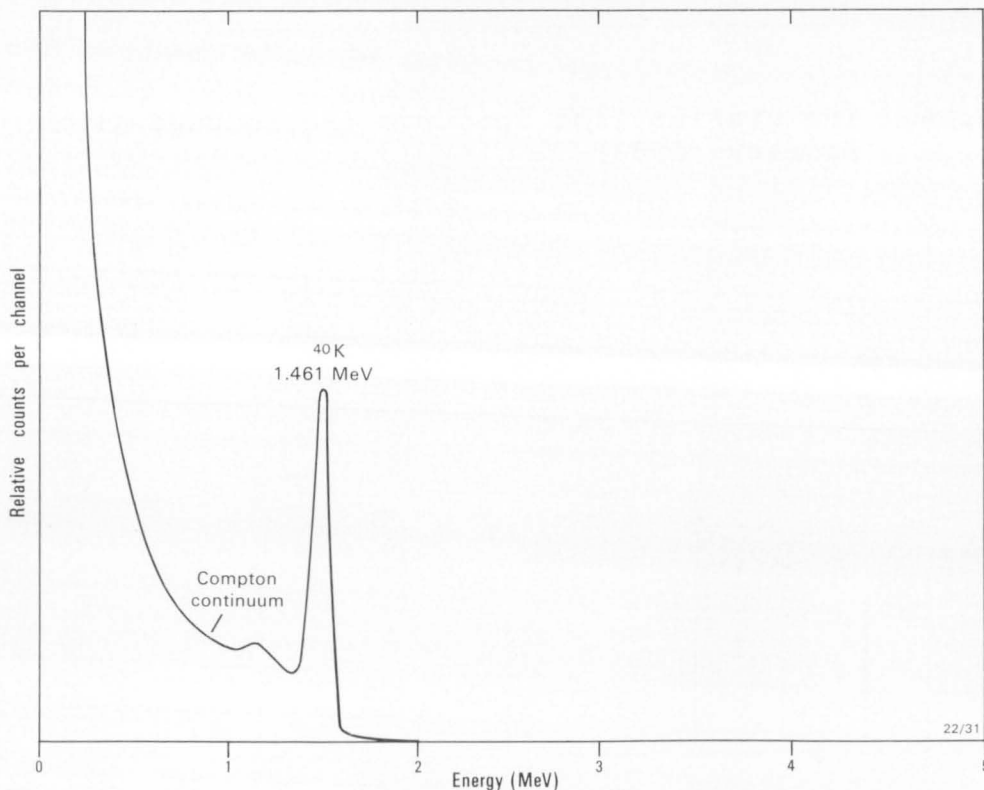
Fig. 7.   The potassium gamma energy spectrum
          (after Fritzsche, 1982).
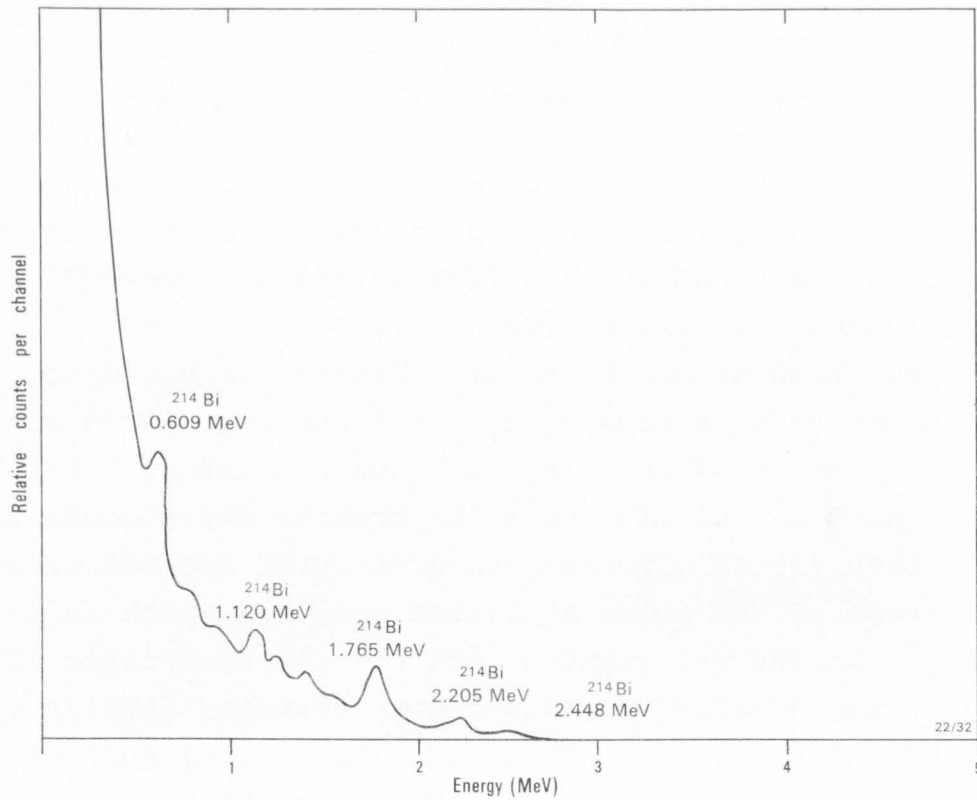
Fig. 8.   The uranium gamma energy spectrum
(after Fritzsche, 1982).
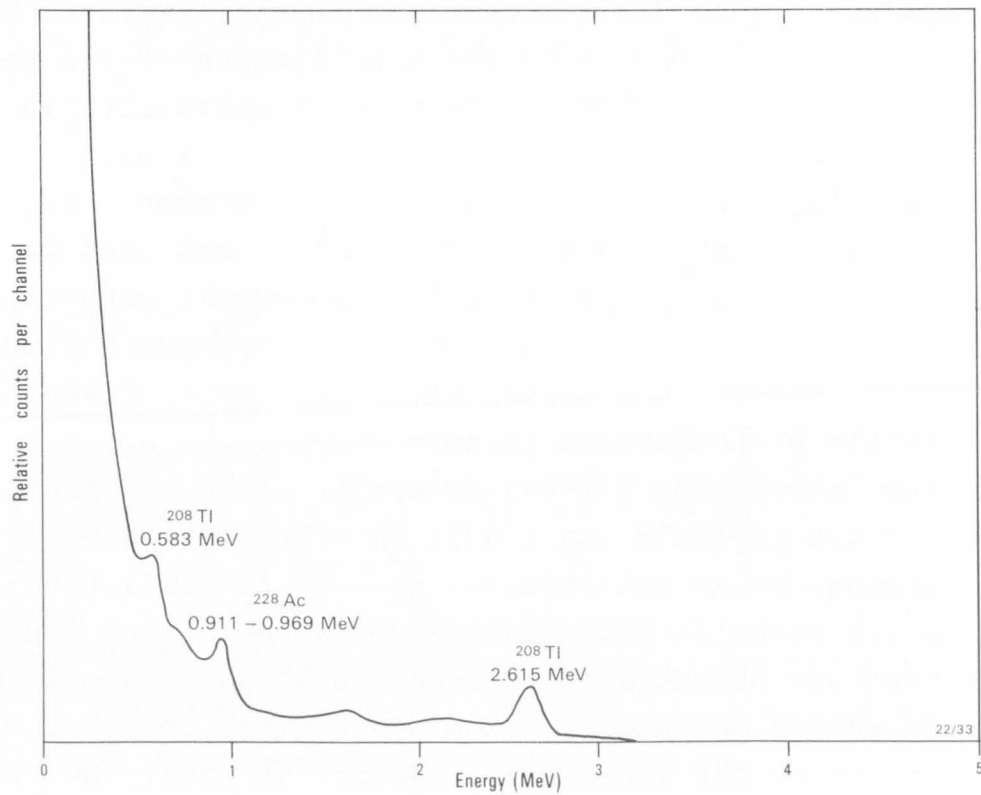
Fig. 9.   The thorium gamma energy spectrum
(after Fritzsche, 1982).

detector a directional sensitivity.

Detector resolution is a measure of a detector's ability to distinguish between two gamma-rays of only slightly differing energy, and in airborne gamma-ray spectrometry it is usually defined as the width of the 0.662 MeV ^{137}Cs peak at half the maximum amplitude, divided by 0.662.

Dead time refers to the finite time required for the spectrometer to process individual photons. This should be as small as possible, since the total counting time available is reduced by the time taken to process all photons detected.

Heath (1964) gives a good summary of **factors affecting the shape of the pulse amplitude spectrum**, such as escape events, accidental summing, and the characteristic 'Compton edge', representing maximum energy transfer between the photon and a recoil electron (Figure 10). Some photons may escape the detector after being only partially absorbed, and their interaction would result in a measured energy somewhat lower than that of the incident photon ('Compton scatter escape'). In each 'pair-production' event, two 0.51 MeV gamma-rays are produced by the annihilation of the positron. Escape of either or both of these photons results in recorded pulses with energies 0.51 MeV and 1.02 MeV less, respectively, than that of the incident photon ('pair-production escape'). This effect can lead to recognisable 'escape peaks' in the spectrum, with energies either 0.51 MeV or 1.02 MeV lower than prominent photopeaks. A similar effect occurs when the 28 keV X-ray given off during the photoelectric process escapes the crystal without further interaction ('X-ray escape'). Also, pair production outside the crystals can result in either or both of the 0.51 MeV photons being detected, to produce 'annihilation radiation peaks'. Note that the photopeaks in a typical spectrum are essentially Gaussian in shape. This is mostly due to energy degradation from scattering, together with absorption on the low-energy side of the peak, and the effect of 'accidental summing' on the high-energy side of the peak. The latter effect is due to the accidental time-coincidence between events occurring in the detector, and the measured spectrum is sometimes referred to as a 'random sum spectrum'.

(b) **Source geometry.** Both source thickness and source type (i.e.
point, line, or broad) affect the shape of the observed
spectrum. Gregory & Horwood (1961) showed that with
increasing source thickness there is a greater build-up of
the Compton continuum. The photopeaks - which are the
distinguishing characteristic of all spectra - are reduced

MONOENERGETIC GAMMA-RAY SOURCES
USED TO DETERMINE RESPONSE

Nuclide	Energy (Mev)	Nuclide	Energy (Mev)
Te 129m	0.109	Y 91m	0.555
Sc 47	0.155	Cs 137	0.662
Ru 97	0.213	Nb 95	0.764
Xe 135	0.250	Mn 54	0.835
Hg 203	0.279	Nb 92	0.930
In 115m	0.335	Zn 65	1.114
In 113m	0.393	A 41	1.290
Au 198	0.411	V 52	1.430
Be 7	0.478	K 42	1.510
Sr 85	0.513	Al 28	1.780
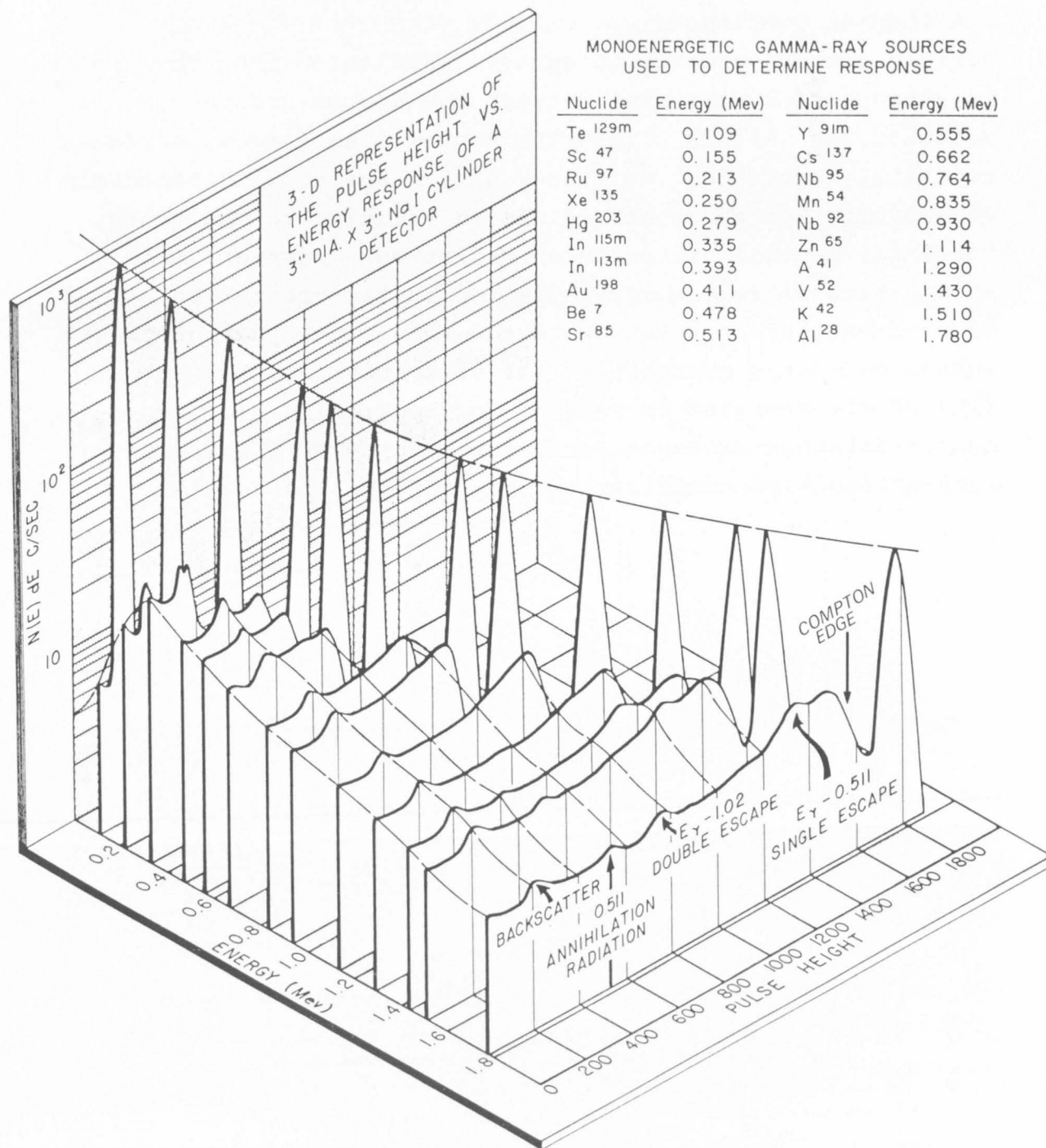
Fig. 10. Pulse height vs. energy response of an NaI
detector (Reproduced from Heath, 1964).

relative to the Compton background, with a consequent lack of resolution, particularly in the low-energy region where the build-up due to Compton scattering is greatest. A similar change in spectrum shape is seen between spectra due to point and broad sources - i.e. with broad sources, greater Compton scattering in the sources themselves results in a build-up of the Compton continuum.

(c) **Terrain clearance/cover thickness.** Radiation from the ground is attenuated by material between the source and the detector, as well as within the source itself (e.g. barren regolith, vegetation, moisture, air). Again, with increasing attenuation the photopeaks diminish relative to the energy continuum because of scattered radiation. However, the attenuation of low-energy radiation is far greater than that of high-energy radiation, with the result that even with increased energy degradation due to scattering, the total flux at all energies is reduced for increasing source-detector distances or increasing cover (Fig. 11). Mass-attenuation coefficients and half-thicknesses for
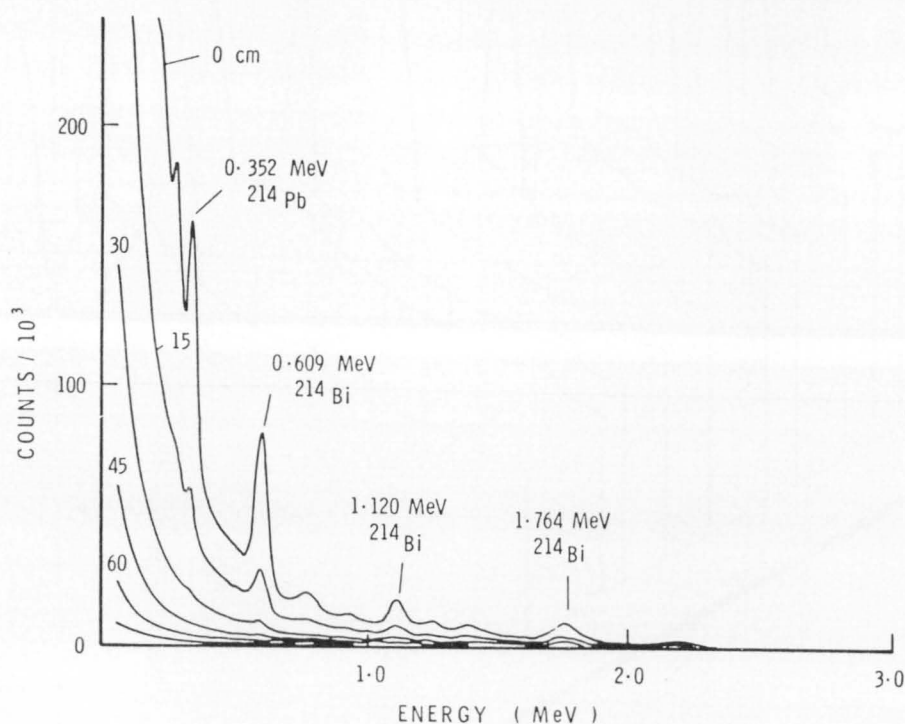
Fig. 11.   Spectra from uranium ore covered by various depths of water (Reproduced from Dickson & others, 1979).

various gamma-ray energies in air, water, terrain clearance and
concrete are given in Table 4 (Grasty, 1979). The effect of
terrain clearance/cover thickness on total flux is also
important:

- just 2 cm of barren regolith will reduce by 35 percent
  the radiation penetrating to the ground surface
- an increase in soil moisture of 10 percent will decrease
  the radiation flux by about 10 percent
- at a terrain clearance of 150 m, a change in altitude of
  15 m will produce a 10 percent change in measured
  radiation
- air density can change by up to 30 percent with changing
  temperature, pressure, and humidity, and this leads to a
  corresponding change in height correction factors
- in some areas, dense vegetation would be equivalent to
  50 m of air in its capacity to shield radiation
- owing to attenuation within the source, the vast majority
  of photons detected originate in the top 35 cm of the
  Earth's crust.

The preceding discussion illustrates that the measured
spectrum is a complex function of many variables and thus defies
analytical description. The approach taken to calibration,
therefore, is empirical, that is, we view the source and detector
as a single system and measure its response, for example, to
variations in source concentration (to obtain channel interaction
corrections) and to changes in aircraft altitude (to obtain
attenuation coefficients). It is important to realise, however,
that these empirically determined constants are only valid for
the source and source-detector geometries used in the calibration
process.

PROCESSING

Drift correction (or 'energy calibration')

All spectrometers are affected by energy drift in the
measured spectra. This is due mainly to changes in the gains of
the photomultiplier tubes (PMTs) because of drift in the high-
voltage supply and changes in temperature. Modern methods of

control include the incorporation of a reference isotope or
artificial light source within each detector package, to enable
the gain of the system to be kept constant through automatic
adjustment of the high-voltage supply to the PMTs. This is
probably the best method of drift control.

Systems without automatic drift adjustment will suffer a loss
of photopeak resolution when individual detectors (i.e., crystal
+ PMT) do not drift sympathetically. Grasty & others (1985) and
Grasty (1982) describe a multichannel processing technique for
correcting for drift on these systems, using the entire spectrum.
This is an improvement on techniques using the potassium
photopeak (1.46 MeV), which can drift into lower energy channels
for anomalously high thorium concentrations.

Dead time correction

Owing to design limitations, spectrometers require a finite
time to process each pulse from the detector. Any pulse that
arrives while another is being processed is automatically
rejected and the total counting time available is thus reduced by
the time taken to process all pulses detected. High countrates
due to large crystal volumes or areas of high radioelement
concentration can thus lead to considerable errors. A typical
'dead' time would be of the order of 5-15 μs/pulse, and can be
corrected for as follows:

$$N = \frac{n}{1 - nt}$$

where N = true counts per second, n = observed counts per
second, and t = dead time in seconds.

Darnley & Grasty (1972) found experimentally that dead time
reduced the thorium height correction coefficient (see Altitude
Correction, below) by as much as 15 percent in areas of high
radioelement concentration.

A method for estimating the dead time of an instrument is
described by van Rooyen (1979). Bristow (1983) describes
hardware modifications that allow for an automatic correction for
dead time.

Background corrections

The contribution of background radiation to the observed spectrum must be subtracted, and can be estimated in a number of ways:

(a) The radiation level can be recorded at **a terrain clearance of 1000 m** before and after each survey flight. At this clearance almost all terrestrial radiation is absorbed by the atmosphere and the observed spectrum can be considered as background. The assumption here is that the cosmic and radon contributions to the total background are the same at 1000 m as at the survey terrain clearance (150 m). This is not necessarily the case. BMR tests (Wilkes, 1976) showed that background estimates at 900 m were 10-15% higher than measurements at 150 m over water. It must also be assumed that the background varies linearly with time between the start and end of the flight and that radon effects are space-invariant. Again, these are known to be only poor approximations. For example, large fluctuations in cosmic background over a few hours are known during periods of solar activity (Korff, 1964), and Darnley & Grasty (1971) note that atmospheric radioactivity can vary considerably between sites only a few kilometres apart.

(b) A better method of determining background is to record the radiation level while flying over **a large body of water** at the survey terrain clearance, since gamma rays are almost completely attenuated by about 1 m of water. This is the approach favoured in Canada where the frequent distribution of lakes is such that background values can be updated several times during a flight. This method is impractical if suitable bodies of water are not available in the survey area (as, e.g., throughout most of Australia), and, again, it must be assumed that the background varies linearly with elapsed time between background determinations, and that radon effects are space-invariant.

(c) In larger aircraft it is possible to have an **'upward-looking' detector** to monitor the background level of radiation continuously. These systems have an additional crystal pack shielded from radiation from below. Foote (1969) used 10 cm

of lead to shield the detector from below, but this weight penalty could be serious for some survey aircraft. The reduction procedure is fairly complex - details are given in Appendix 1. The procedure requires that the detector system be configured with a 3.0-6.0 MeV 'cosmic channel' to monitor the contribution of cosmic background and to allow the calculation of aircraft background. With this extra 'cosmic' channel it is possible to calculate the cosmic background contribution at every sample, without recourse to an upward-looking detector. Applying this to methods (a) and (b) above for single detector systems results in the interpolated backgrounds being used only to estimate the radon contribution to total background.

(d) **Full spectrum analysis** using multichannel data includes the possibility of estimating the amount of background ^{214}Bi and ^{214}Pb in the air and thus avoiding the use of upward-looking detectors. Bristow (1983) has suggested that, if detector resolution improved to the point where ^{214}Bi photopeaks at 0.609 and 1.12 MeV, for example, could be satisfactorily resolved, then it may be possible to distinguish airborne ^{214}Bi signals from terrestrial ones by their different spectral shapes. A comparison of Figures 2 and 8 illustrates how the spectrum due to airborne radiation suffers less attenuation of the lower-energy photopeaks relative to the one at 1.76 MeV, and less Compton scatter build-up in the low-energy portion of the spectrum. Grasty (1982) reports a good correlation between the ^{214}Pb gamma-ray peak at 0.352 MeV and the standard uranium window (^{214}Bi at 1.76 MeV) for background flights over lakes. Since low-energy 0.352 MeV gamma rays are almost completely absorbed by 150 m of air, it is possible they might be useful for monitoring atmospheric radioactivity. This would be the best solution, since no assumptions need to be made about the spatial distribution of airborne radioactivity. The use of upward-looking detectors assumes that vertical mixing of the airborne radioelements has resulted in an even distribution of these sources in the vicinity of the detector.

Terrain-clearance correction

Airborne radiometric data need to be corrected to a nominal survey terrain clearance to remove the effect of variations in terrain clearance. Attenuation of radiation with distance depends on the geometry of the source as well as on the energy of the radiation. Thus, the radiation from narrow sources attenuates more rapidly with distance than that from broad sources, and low-energy radiation falls off more rapidly with distance than high-energy radiation.

A gross correction for terrain clearance can be obtained by considering an exponential fall-off of radiation as a function of the instantaneous terrain clearance (Darnley, 1972):

$$N = N_o e^{-u(H-h)}$$

where u = the empirically derived attenuation coefficient for any particular energy interval and a particular source type

N_o = the observed countrate at terrain clearance h

N = the corrected countrate for the nominal survey terrain clearance H

This algorithm is adequate for subdued topography and ground clearances in the range 50-250 m. More accurate algorithms are given by Godby & others (1952) and GeoMetrics (1974). The latter algorithm was discussed by Minty (1977a) and gives a more comprehensive correction in rugged topography by considering the two-dimensionality of the source. It should be emphasised that there is no exact ground clearance correction, as all methods must make some necessarily arbitrary assumptions about the source geometry.

Wilkes (1976) describes experimental studies undertaken at the BMR and notes that empirically determined attenuation coefficients depend on the relative radioelement concentrations of the source as well. For example, attenuation coefficients measured over a test strip with abnormally high thorium content will produce lower than normal attenuation coefficients for the

uranium and potassium channels (for a three-channel system), owing to increased scatter into the lower-energy channels. A further complication is that the density of air (and thus the attenuation coefficients) is a function of temperature and pressure. While pressure differences produce maximum changes in the attenuation coefficient of only 1-2 percent, temperature changes produce about 3 percent change per 10 degrees Centigrade temperature difference (Wilkes, 1976). The method used by the Geological Survey of Canada to accommodate temperature/pressure changes is described in Appendix 2.

The most that can be expected of a ground clearance correction is an improvement in the quality of the data. Furthermore, beyond a certain maximum clearance (perhaps 300 m), the gamma radiation is almost completely attenuated by the air. It is therefore unrealistic to attempt to correct the recorded countrates once a certain critical clearance is exceeded.

Reduction to elemental countrates

This correction is also known as the 'channel interaction correction' or 'stripping correction'. Once the observed gamma-ray spectrum has been corrected for background, ground clearance, dead time, and spectrometer drift (for multichannel systems), it is necessary to determine what contribution (in terms of countrates) each of the three fundamental elements (K, U, and Th) makes towards the observed spectrum. A brief summary of the least-squares matrix method of analysis is given in Appendix 3. This method can be applied to data acquired by either conventional three-channel spectrometers or multi-channel spectrometer systems.

From a qualitative point of view the reduction procedure could be described as follows:

(1) The response of the system to different sources of known composition is observed for a fixed source-detector geometry considered representative of survey conditions. By suitable choice of sources, these data can be used to calculate the spectra that would be observed by the system for pure sources of K, U, and Th. Usually, large, radioactive-concrete calibration pads are used to simulate broad sources of

infinite thickness (Grasty, 1979), and plywood sheets are used to simulate the absorption of gamma radiation in the air (Dickson, & others, 1981).

(2) These responses are then normalised for each pure source, such that the total number of counts over all channels is unity.

(3) The actual counts due to K, U, and Th are then found by determining the linear combination of the three 'pure' response functions that will give the best approximation to the observed spectrum, i.e., by solving the relationship:

observed spectrum =

counts due to Th x pure Th response function
+ counts due to U x pure U response function
+ counts due to K x pure K response function

Thus the total number of counts detected over the observed spectrum is subdivided into counts due to the three radioelements.

Conversion of countrates to elemental abundances

Gamma-ray spectrometric data are often denoted in counts per unit time (countrates). This is undesirable because the countrates are dependent not only on the ground radioelement concentration, but also on the equipment used, and on the reference altitude (nominal terrain clearance) of the particular survey. Crystal volume, detector efficiency, and spectrum width will all affect the observed countrate and make it difficult to compare results from two different surveys. It is thus desirable that survey measurements be expressed in terms of mean-ground-level abundances of the respective elements.

The problem can be approached in two ways, depending on the level of accuracy required. The Geological Survey of Canada's approach (Darnley & Grasty, 1971) is via calibration flights at known heights over a carefully selected test strip. The test strip has reasonably uniform concentrations of the radioelements which have been determined by systematic ground sampling and chemical analysis. For a specific ground clearance and survey

system, a factor is calculated that will convert countrates to element abundances, e.g., 1 ppm U = n counts/s.

This method is usually sufficient, although small errors can occur in areas of high radiometric gradients where anomalous ground concentrations will appear broader in extent than they really are.

Alternatively, a linear inverse technique (Minty, 1977b) could be employed (Appendix 4). This technique theoretically gives a better indication of ground-level concentrations by considering more than one data point in the evaluation, but at the cost of increased computer time. Similar techniques are described by Gunn (1978) and Crossley & Reid (1982), although Gunn (1978) has suggested that the quality of data required for this type of analysis is still beyond the capability of modern spectrometer systems. All methods require the use of a well-sampled test strip.

Filtering of statistical noise

The inherent 'noise' in gamma-ray spectrometric data is predicted by statistical sampling theory, and is sometimes called the statistical noise.

It arises because we are using a finite sampling interval to sample events (radioactive decays) that are occurring at random intervals. Fortunately the main frequency content of the noise is much higher than that of the signal, and the noise can be removed by filtering. The use of a cross-correlation (matched) filter for gamma-ray spectrometric data has been discussed by Richards (1977b). Tammenmaa & others (1976) used Fourier analysis to design optimum filters and to show that the decreased signal-to-noise ratio arising from a shorter measurement time can be regained by the application of a suitable filter. Bristow (1983) reviews the application of signal extraction techniques to gamma-ray spectrometric data-processing in some detail.

DISCUSSION AND CONCLUSIONS

Automatic estimation of attenuating cover

As noted already, the effect on the observed spectrum of an increase in thickness of attenuating material between the source and the detector, is that the photopeaks diminish relative to the energy continuum spectrum, owing to scattered radiation, with a consequent lack of resolution - particularly at lower energies where the build-up due to Compton scattering is greatest. This, in turn, changes the calibration constants required to convert the observed spectrum to elemental countrates. It is thus of some interest to note that Dickson & others (1979) developed a technique for correcting for overburden effects in surface surveys of uranium orebodies, by essentially measuring ^{214}Bi photopeaks as a ratio of the Compton continuum in their vicinity. This two-channel technique can estimate cover up to 45 cm thick if counting times are long enough.

Dickson (1980) and Dickson & others (1981) extended this concept, to use the change in shape of the entire spectrum in order to estimate the thickness of intervening absorbing material. They used a principal-component analysis of spectra obtained from sources under variable cover to show that the spectrum of each of the three radioelements is composed of two spectral components that can be summed in predictable proportions for a given thickness of absorbing material. Unfortunately, the method at present requires large countrates to be accurate, and is thus impractical for airborne systems. However, it is immediately applicable to multichannel ground surveys, and holds exciting possibilities for airborne data analysis should improved detector efficiencies and processing procedures make this possible.

Minimising errors: optimising the processing options

Equilibrium and background considerations aside, there are three aspects to minimising errors in the reduction of the data. These are (1) statistical noise, (2) the 'condition' of the system of equations used to reduce the data to elemental countrates, and (3) the sensitivity of this system to variations in the source-detector geometry. Here, source-detector geometry

includes the effects of finite sources at variable distances from the flight line, angular sensitivity of the detector, source thickness, and variations in thickness of attenuating cover.

Minty (1978) and Grasty & others (1985) have shown that, for multichannel spectrometers, statistical errors are minimised by including all channels in the analysis. In fact, Grasty & others (1985) show that, for 172 channels and weighting each channel according to the variance of its countrate, significant reductions of up to 25 percent in statistical errors can be obtained. However, it would be wrong to conclude that the errors in elemental abundances are reduced by this amount compared to the three-window method, since their analysis ignores the effect of the condition of the system of data-reduction equations and variations in the source-detector geometry.

Certain systems of linear equations are more suitable than others for solving for the unknowns, and a measure of this (the 'condition number') is the ratio of the smallest to the largest eigenvalues of the system (McSharry, 1973). For well-conditioned systems, the condition number approaches 1, and for poorly conditioned systems it approaches 0. Thus the condition number of a calibration matrix for a particular selection of channels gives an indication of how well suited that system is to the task of determining each element's contribution to the observed spectrum - without considering other relevant factors such as count statistics, source geometry, etc. McSharry (1973) did this for various three-channel systems and concluded that Grasty & Darnley's (1971) window configuration was the best-conditioned of the common systems used at that time, but warned that changing windows for better counting statistics may not make up for inaccuracies lost by the use of poorly conditioned systems.

Crossley & Reid (1982) present a matrix method of obtaining a measure of the inversion importance of each channel for a particular calibration matrix. Their analysis shows that photopeaks have greater inversion importance, which is not suprising considering that these are the distinguishing characteristics of all spectra. They also concluded that, for surveys with a limited number of channels, the addition of low-energy uranium and thorium windows (centred at 0.94 MeV for Th and 1.12 MeV for U) may improve abundance estimation

significantly. However, their analysis used calibration data acquired at ground level using point sources, and these photopeaks are less well resolved for broad sources at survey altitude. Their approach also ignores the contribution of counting statistics and source geometry to the accuracy of the estimated abundances. Nevertheless, this study provides a useful insight into optimum channel selection for minimising errors due to ill-conditioning in the matrix inversion technique.

Future research should focus on the integrated effects (on the accuracy of estimated abundances) of count statistics, system conditioning, source-detector geometry, disequilibrium, and errors in background estimation. For example, the preferential weighting of high-count, low-energy channels in the reduction procedure to minimise statistical errors ignores the fact that these channels may have far less inversion importance than higher-energy channels of lower countrate. In addition, the higher-energy part of the spectrum is less susceptible to variations in the source-detector geometry owing to the greater penetration of radiation at these energies.

The conventional windows for three-channel systems, centred on 1.46 MeV (K), 1.76 MeV (U) and 2.62 MeV (Th) (Table 5) were originally chosen because they are centred on the highest-energy diagnostic photopeaks of each of the three radioelements. Further research may well indicate that this configuration is near optimum.

Background estimation

Full spectrum analysis using multichannel data would be the best approach to atmospheric background estimation, since no assumptions about the spatial distribution of sources need be made. However, further research is required in order to determine the feasibility of this approach using present systems.

An upward-looking detector system is the only current alternative for obtaining regular background estimates in areas where frequent 'over-water' backgrounds are impossible. There is very little documentation on the reliability of this technique other than Figures 12 and 13 extracted from Fritzsche (1982) and showing a spread of about ± 10 percent in calculating the sensitivities ℓ and m (see Appendix 1). The condition of this

system might be improved by using lead to more effectively shield
the upper detector from radiation from the ground. This would,
however, increase the proportion of annihilation radiation
detected in both detectors because of the high cross-section lead
has for pair production.

Both methods should include a high-energy 3.0-6.0 MeV window
for calculating cosmic background. There seems little point in
including cosmic background in the inversion procedure when it
can be independently monitored and is known to vary relatively
slowly with time.
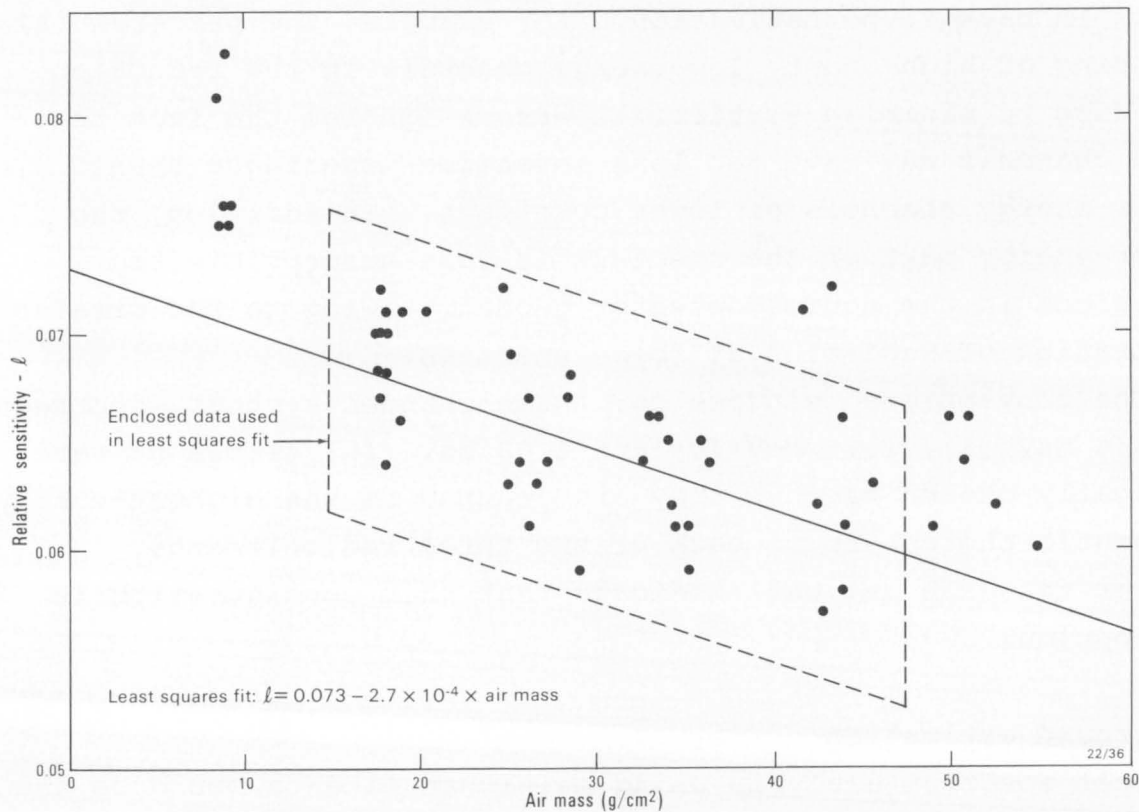
Fig. 12. The relative sensitivity of the up detectors to
the down detectors for terrestrial gamma
radiation (after Fritzsche, 1982).

Least squares fit: m = 0.291 − altitude/4419

22/37

Relative sensitivity-m

Altitude (metres)
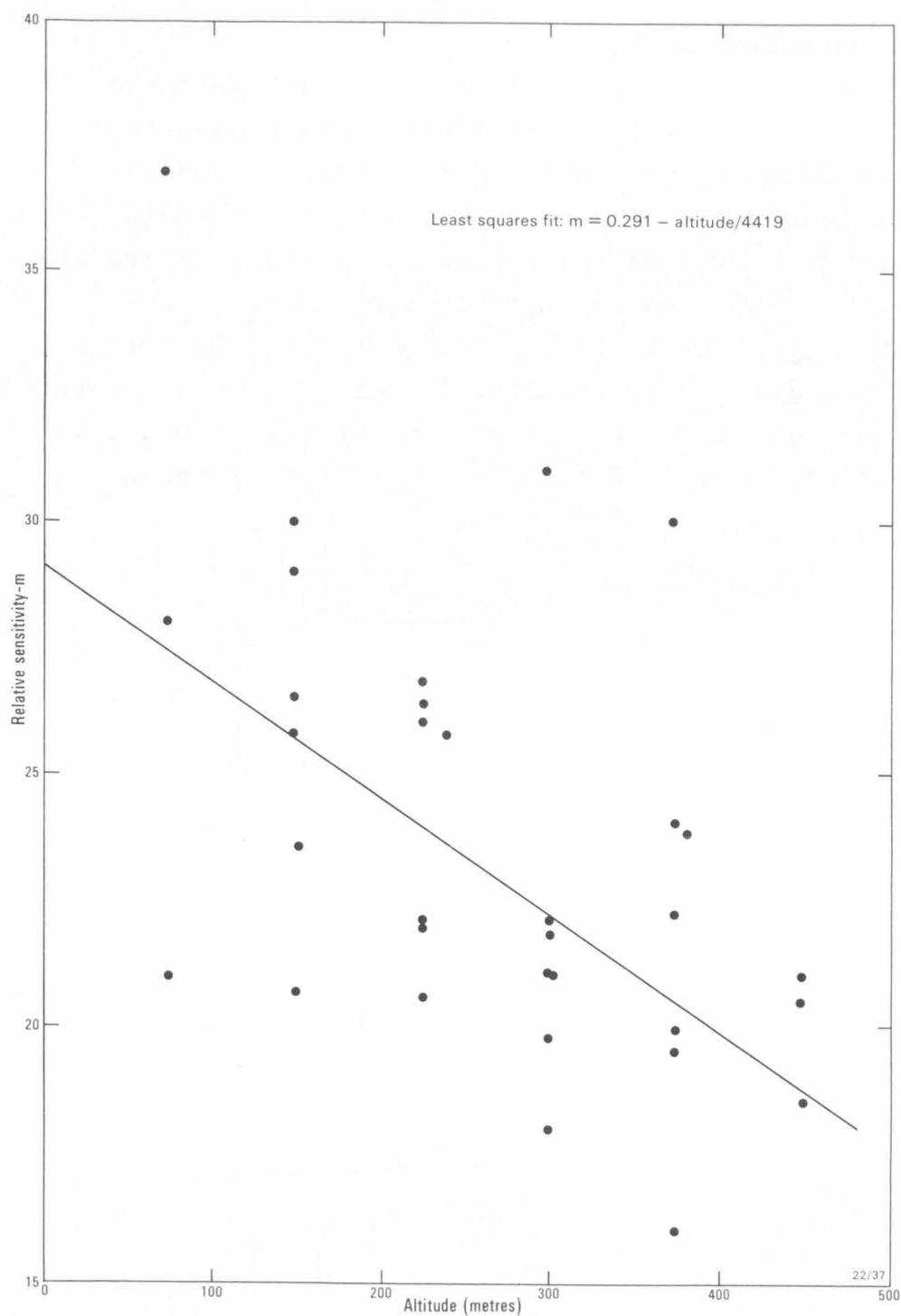
Fig. 13.   The relative sensitivity of the up detectors to
the down detectors for airborne radon (after
Fritzsche, 1982).

Coincident detection technique

Duckworth (1983) has proposed a coincident detection technique which would allow directional detection of radiation without shielding, using a pair of detectors acting in coincidence (Fig. 14). The concept relies on the coincident detection in the lower detector of photons backscattered by the upper detector. This concept might also be used for 'unscattering' backscattered radiation detected in this way and which normally would have resulted in some photopeak degradation due to Compton scatter escape in the upper detector. This technique has not yet been tested on airborne systems.

Fig. 14. Use of a coincident detection technique to allow directional detection of radiation (Reproduced from Duckworth, 1983).

RECOMMENDATIONS

(1) It is essential, for system calibration, to have access to standard calibration sources of known element abundances. The conventional approach is to have large, suitably doped concrete pads simulating thick, broad sources and accessible to aircraft. However, such pads are expensive to build and depend on the availability of a suitable site at a convenient airfield. It is recommended that consideration be giv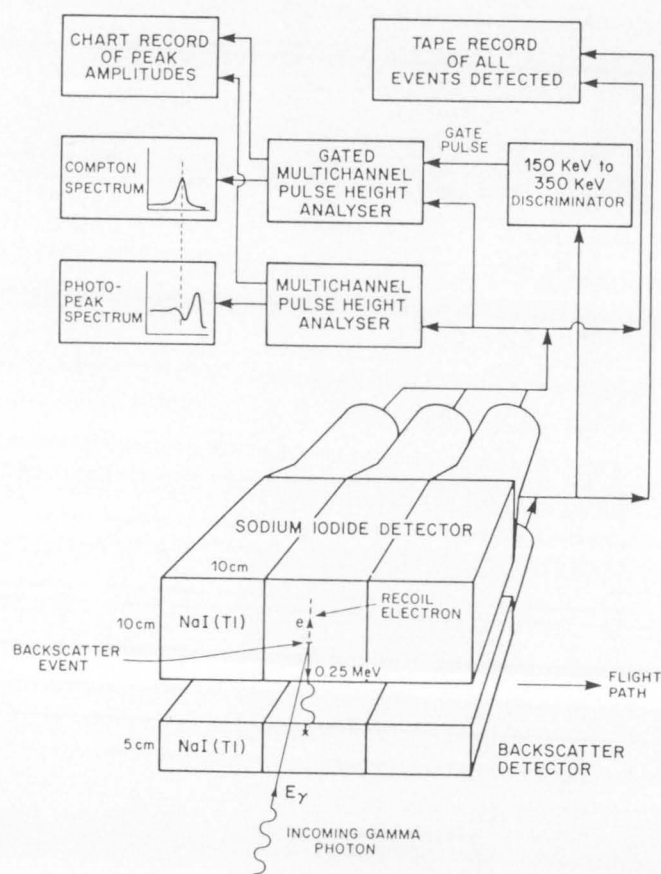en to a compromise solution of building portable standards to simulate thick point sources. With suitable lateral shielding, and by integrating the response of the system to various source-detector geometries, these could be used to simulate broad sources for calibration purposes. By using plywood to simulate attenuating material, the portable standards would have the advantage of allowing the response of the system to variable attenuation to be measured with the spectrometer system mounted in the aircraft. This method would also provide valuable finite source data, using variable source-detector geometries for empirical studies into optimum processing procedures.

(2) Consideration should be given to acquiring multichannel data on a routine basis. This would allow frequent energy calibration during processing, and provide flexibility and the ability to reprocess data at a later stage, should future research allow improved processing.

(3) A 3.0-6.0 MeV cosmic window should be added to the present BMR system, to allow continuous monitoring of cosmic background and estimation of atmospheric background using upward-looking detectors.

(4) Temperature and pressure are continuously recorded on BMR surveys. These data should be used during the ground clearance correction procedure, to reduce the data to a standard temperature and pressure along the lines indicated in Appendix 2.

(5) Further research should be conducted into optimising the processing of gamma-ray spectrometric data. This should focus on the integrated effects of count statistics, system conditioning, source-detector geometry, disequilibrium, and

errors in background estimation, on the accuracy of estimated abundances.

ACKNOWLEDGMENTS

REFERENCES

BOTT, M.H.P., 1967 - Solution of the linear inverse problem in magnetic interpretation with application to oceanic magnetic anomalies. Geophysical Journal of the Royal Astronomical Society, 13, 313-323.

BRISTOW, Q., 1983 - Airborne gamma-ray spectrometry in uranium exploration. Principles and current practice. International Journal of Applied Radiation & Isotopes, 34(1), 199-229.

CHARBONNEAU, B.W., & DARNLEY, A.G., 1970 - Radioactive precipitation and its significance to high sensitivity gamma-ray spectrometer surveys. Geological Survey of Canada, Paper 70-1, part B, 32-36.

CROSSLEY, D.J., & REID, A.B., 1982 - Inversion of gamma-ray data for element abundances. Geophysics, 47, 117-126.

DARNLEY, A.G., 1972 - Airborne gamma-ray survey techniques. In URANIUM PROSPECTING HANDBOOK. Institution of Mining & Metallurgy, London, 174-211.

DARNLEY, A.G., & GRASTY, R.L., 1971 - Mapping from the air by gamma-ray spectrometry. In Geochemical Exploration. Canadian Institute of Mining & Metallurgy, Special Volume 11, 485-500.

DARNLEY, A.G., & GRASTY, R.L., 1972 - Airborne radiometric survey of the Fort Smith area. Geological Survey of Canada, Open File 101.

DICKSON, B.H., 1980 - Analytic methods for multichannel airborne radiometrics. M.Sc. thesis, University of Toronto (unpublished).

DICKSON, B.H., BAILEY, R.C., & GRASTY, R.L., 1981 - Utilising multichannel airborne gamma-ray spectra. Canadian Journal of Earth Sciences, 18, 1793-1801.

DICKSON, B.L., CLARK, G.J., & McGREGOR, B.J., 1979 - Technique for correcting for overburden effects in ground level radiometric surveys of uranium orebodies. Geophysics, 44, 89-98.

DUCKWORTH, K., 1983 - Energy discriminant coincidence detection as a possible aid to improved performance in airborne radiation detectors. Geoexploration, 21, 171-179.

FOOTE, R.S., 1969 - Improvements in airborne gamma-radiation data analyses for anomalous radiation by removal of environmental and pedologic radiation changes. In Nuclear techniques and mineral resources. I.A.E.A., Proceedings Series, 187-196.

FRITZSCHE, A.E., 1982 - The National Weather Service gamma snow system - physics calibration. Report by Geo-Metrics to National Oceanic & Atmospheric Administration/National Weather Service, by contract with the United States Department of Energy.

GEO-METRICS, 1974 - High resolution airborne gamma-ray spectrometry - data corrections and applications to geophysical exploration. Geo-Metrics preliminary technical memo, 1974.

GEO-METRICS, 1979 - Aerial gamma ray and magnetic survey, Powder

River R+D Project: Final report prepared for the Department of Energy, Grand Junction Office, Grand Junction, Colorado.

GODBY, E.A., CONNOCK, S.H.G., STELJES, J.F., COWPER, G., & CARMICHAEL, M., 1952 - Aerial prospecting for radioactive minerals. National Research Council Laboratories, Ottawa, Report AECL 13.

GRASTY, R.L., 1975 - Uranium measurements by airborne gamma-ray spectrometry. Geophysics, 40, 503-519.

GRASTY, R.L., 1979 - Gamma ray spectrometric methods in uranium exploration - theory and operational procedures. Paper 10B in Geophysics and geochemistry in the search for metallic ores. Geological Survey of Canada, Economic Geology Report 31.

GRASTY, R.L., 1982 - Utilizing experimentally derived multi-channel gamma-ray spectra for the analysis of airborne data. Symposium on Uranium Exploration Methods; (review of the NEA/IAEA R+D programme). NEA/IAEA, Paris.

GRASTY, R.L., & DARNLEY, A.G., 1971 - The calibration of gamma-ray spectrometers for ground and airborne use. Geological Survey of Canada, Paper 71-17.

GRASTY, R.L., GLYNN, J.E., & GRANT, J.A., 1985 - The analysis of multichannel airborne gamma-ray spectra. Geophysics, 50, 2611-2620.

GREGORY, A.F., 1960 - Geological interpretation of aeroradiometric data. Geological Survey of Canada, Bulletin 66.

GREGORY, A.F., & HORWOOD, J.L., 1961 - A laboratory study of gamma-ray spectra at the surface of rocks. Department of Energy, Mines & Resources, Ottawa, Mines Branch Research Report R85.

GUNN, P.J., 1978 - Inversion of airborne radiometric data. Geophysics, 43, 133-143.

HEATH, R.L., 1964 - Scintillation spectrometry. Gamma-ray spectrum catalogue, 2nd Edition, Volumes 1 and 2: U.S.A.E.C. Research and Development Report IDO-16880-1, Physics T.I.D. - 4500 (31st Edition).

HUBBELL, J.H., & BERGER, M.J., 1968 - Attenuation coefficients, energy absorption coefficients, and related quantities.

ENGINEERING COMPENDIUM ON RADIATION SHIELDING, 1.
Springer Verlag, Berlin.

KORFF, S.A., 1964 - Production of neutrons by cosmic radiation. In ADAMS, J.A.S., & LOWDER, W.M. (Editors) - THE NATURAL RADIATION ENVIRONMENT. University of Chicago Press, Chicago. 427-440.

LARSON, R.E., & HOPPEL, W.A., 1973 - Radon-222 measurement below 4 km as related to atmospheric convection. Pure & Applied Geophysics, 105(4), 900-906.

LOVBORG, L., BOTTER-JENSON, L., & KIRKEGAARD, P., 1978 - Experiences with concrete calibration sources for radiometric field instruments. Geophysics, 43, 543-549.

McSHARRY, P.J., 1973 - Reducing errors in airborne gamma-ray spectrometry. Bulletin of the Australian Society of Exploration Geophysicists, 4(1), 31-41.

MINTY, B.R.S., 1977a - Correction of airborne radiometric data for variations in the terrain clearance of the detector. Geological Survey of South Africa, Open File Report 50.

MINTY, B.R.S., 1977b - A preliminary report on a matrix method of solving the linear inverse problem in radiometrics. Geological Survey of South Africa, Open File Report 57.

MINTY, B.R.S., 1977c - The weighted least squares analysis of n-channel spectrometer data. Geological Survey of South Africa, Report Gh2413.

MINTY, B.R.S., 1978 - An error analysis for multichannel gamma-ray spectrometers. Geological Survey of South Africa, Report Gh2457.

RADIOLOGICAL HEALTH HANDBOOK, 1970 - United States Bureau of Radiological Health. Public Health Service Publication 2016.

RICHARDS, D.J., 1977a - Extension of gamma-ray spectrometer calibration to multichannel spectrometers with application to Karoo Airborne Geophysical Survey. Geological Survey of South Africa, Report Gh2252.

RICHARDS, D.J., 1977b - Karoo uranium occurrences - modelling of the airborne gamma-ray spectrometer response for digital cross-correlation filtering of observed profiles and removal of statistical noise. Geological Survey of South Africa, Open File Report 67.

RICHARDS, D.J., SIMON, I., O'SULLIVAN, K., & HOGAN, A., 1983 - An image processing system applied to airborne radiometric data. <u>Abstracts, 3rd A.S.E.G. Biennial Conference, Brisbane, 1983</u>, 150-152.

TAMMENMAA, J.K., GRASTY, R.L., & PELTANIEMI, M., 1976 - The reduction of statistical noise in airborne radiometric data. <u>Canadian Journal of Earth Sciences</u>, 13, 1351-1357.

VAN ROOYEN, D.W., 1979 - Instrumentation as applied to source material exploration. Training course on radiometric prospecting techniques, Pelindaba, South Africa, 21-23 May 1979; presented by the Atomic Energy Board in collaboration with the South African Geophysical Association and the Geological Society of South Africa.

WILKES, P.G., 1976 - Acquisition, processing, and interpretation of airborne gamma-ray spectrometry data. <u>Bureau of Mineral Resources, Australia, Report</u> 186.

APPENDIX 1

**Background estimation using an upward-looking
detector (after Geo-Metrics, 1979)**

Aircraft and cosmic background

This procedure makes use of the fact that below about 12 km
altitude the cosmic spectrum has a constant shape but its
amplitude decreases with decreasing altitude. Also, above
3.0 MeV all radiation is cosmic in origin. Irrespective,
therefore, of other sources of radiation, the cosmic contribution
in any channel is proportional to the total count between say,
3.0 and 6.0 MeV; i.e., if we know the shape of the cosmic
spectrum for a particular installation, then for each detector we
can use the 3.0-6.0 MeV countrate to calculate the cosmic
contribution in any particular channel.

The stategy is to collect full spectra over water at a number
of different heights (say 1,2, ..6 km) where there is no airborne
^{214}Bi, e.g. offshore where the prevailing winds are landwards,
or alternatively after a high-pressure front arrives, or after
general precipitation in the calibration area, since both tend to
reduce atmospheric radioactivity to low levels (Fritzsche, 1982).
The measured spectra are each the sum of the aircraft component
(constant) and the cosmic component. The cosmic component is
then the difference between any two spectra normalised to the
same 3.0-6.0 MeV countrate. This procedure can be repeated for
each combination of heights and the results averaged. The
aircraft spectrum is obtained by subtracting the cosmic
background spectrum from any of the observed spectra. Again, the
results can be averaged. Geo-Metrics (Fritzsche, 1982) found
that with their system (21 L down detector and 4.2 L up), five
minutes counting time at each height was generally sufficient and
the difference in heights should be at least 1000 m. Fritzsche
(1982) also suggests that a more accurate aircraft background can
be obtained by flying at survey height over water on a low-radon
day and then subtracting the cosmic component.

Atmospheric radon background

Consider the following crystal configuration:
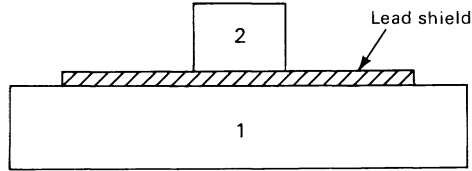
Let 1 and 2 designate the downward-looking and upward-looking crystals respectively. The down crystal 'sees' a radiation rate, I_1, composed of the ground signal, I_g, and the air signal, I_a, plus aircraft (A_1) and cosmic (C_1) background, i.e.

$$I_1 = I_g + I_a + A_1 + C_1$$

Similarly,
$$I_2 = \ell I_g + m I_a + A_2 + C_2$$

where m is the response to the air signal and ℓ is the percentage of the ground signal penetrating through to the upward-looking detector.

For calibration data acquired over suitably doped concrete calibration pads, and after subtracting the background measured over a suitably doped 'background' pad, we have

$$A_1 = A_2 = C_1 = C_2 = I_a = 0$$

Therefore,
$$I_1 = I_g$$

$$I_2 = \ell I_g$$

and
$$\ell = I_2 / I_1$$

Probably a better method of determining ℓ is by flying at different heights from water to land with the water data simply being used to subtract all background.

Note that, owing to 'skyshine' (backscattering of photons by the air), ℓ should decrease with height for broad sources, i.e., $\ell = f(h)$. This height dependence should not be severe for

channels above 1.0 MeV, since the average energy of backscattered radiation is substantially less than 1.0 MeV.

The factor m is calculated from 'over-water' data at survey height when radon + daughters are present. This can be done a number of times for various radon concentrations and the results averaged.

In this case, $I_g = 0$ and A_1, A_2, C_1, and C_2 can be measured and removed as described earlier.

Therefore,
$$I_1 = I_a$$

$$I_2 = m I_a$$

and
$$m = I_2 / I_1$$

Note that m changes with height, since as height decreases, the earth intercepts an increasing fraction of the volume of radioisotope-bearing air and this is more severe for the down detector than the up detector. m is also uncertain because of the unknown shape of the vertical radon concentration profile. This uncertainty can be minimised by ensuring that all calibration and survey flights are flown after air turbulence has mixed the radon vertically in the atmosphere.

Atmospheric background can thus be estimated as follows: both the up and down counting rates are corrected for aircraft and cosmic background, to give

$$I_1 = I_g + I_a$$

$$I_2 = \ell I_g + m I_a$$

or
$$I_a = (I_2 - I_1) / (m - \ell)$$

which is subtracted from the down-channel countrates to give background corrected data.

Figures 12 and 13 show the variation in empirically determined values for m and ℓ for the Geo-Metrics system (Fritzsche, 1982). The data have a spread of ± 10 percent, which illustrates the difficulty in making these measurements. Varying

radon distributions and poor counting statistics probably combine to introduce significant errors.

APPENDIX 2

Temperature and pressure corrections

Consider the radar altimeter reading as an elevation or height. For an ideal gas, the equation of state is

$$pV = nRT, \text{ where}$$

p = pressure (atm), V = volume (litres), n = mass of gas (moles), R = universal gas constant [= 8.314 J/(mole K)], and T = temperature (K).

Substituting 'ha' for the volume of a column of air of height 'h' and cross-sectional area 'a', and solving for the ratio of two values of 'h',

$$p_0 h_0 a = nRT_0 \quad \text{(at STP)}$$

$$p_1 h_1 a = nRT_1 \quad \text{(observed)}$$

$$(p_0 h_0)/(p_1 h_1) = T_0/T_1$$

we get

$$h_0 = (T_0/T_1)(p_1 h_1)/p_0$$

To correct a radar altimeter reading h_1 at pressure p_1 and temperature T_1, to that which would be observed at standard pressure p_0 and temperature T_0,

$$p_0 = 101.325 \text{ kPa (760 mm Hg) and } T_0 = 273.15 \,^{\circ}K \, (0\,^{\circ}C),$$

we use

$$h0 = \frac{(0+273.15)\ (press)\ (altim)}{(temp+273.15)\ (101.325)}$$

where temp = observed temperature (^{O}C), press = observed pressure (kPa), and altim = observed radar altimeter.

This corrected altimeter value is then used with the attenuation coefficients.

APPENDIX 3

Reduction to elemental countrates

The number of photons, R, (due to primary monochromatic radiation) detected per unit time in a particular energy window is generally assumed to be directly proportional to the concentration, x, of surrounding radioactive elements, i.e.,

$$R = ax$$

where a is a proportionality constant. This is the ideal case. The observed countrate is, however, also influenced by absorption and by Compton scattering of rays with energies initially outside the window under consideration. It is therefore necessary to calculate the contribution in each energy window from gamma-rays of all possible sources. For 3 sources and n channels (windows) we can set up the following system of equations:

$$R_1 = a_{11}x_1 + a_{12}x_2 + a_{13}x_3$$
$$R_2 = a_{21}x_1 + a_{22}x_2 + a_{23}x_3$$
$$\cdot$$
$$\cdot$$
$$\cdot \hspace{8cm} (1)$$
$$\cdot$$
$$R_n = a_{n1}x_1 + a_{n2}x_2 + a_{n3}x_3$$

i.e. $\qquad R_i = \sum_{j=1}^{3} a_{ij}x_j \qquad i=1$ to n $(n \geq 3)$ $\qquad$ (2)
$\qquad j=1$ to 3

where R_i = countrate in the ith channel, x_j = concentration
of the jth element (i.e. K, U, or Th), and a_{ij} = proportion of
counts appearing in the ith channel for a given concentration of
the jth element.

In matrix notation, equation 1 can be written as

$$R = AX \qquad (3)$$

which has the least-squares solution (n > 3)

$$A = RX^t(XX^t)^{-1} \qquad (4)$$

The calibration matrix, **A**, is thus calculated by observing
the response of the detector to sources of known composition. The
calibration constants determined will be a function of the
source/detector geometry, crystal size, detector efficiency, and
channel widths.

Richards (1977a) has shown that by suitable normalisation of
the calibration matrix **A** (divide each row by the sum of the
elements in that row), each element of the array will represent
the proportion (in a particular channel) of the total number of
counts (recorded in n channels) due to either potassium, uranium,
or thorium. Equation (3) can thus provide a means of calculating
the unknown total countrates due to each of K, U, or Th,

$$R_i = \sum_{j=1}^{3} a_{ij}x_j \qquad (5)$$

where R_i = countrate in the ith channel

$\qquad x_j$ = total countrate due to jth element (i.e. K, U or Th)

$\qquad a_{ij}$ = the proportion in channel i of the total number of
$\qquad\qquad$ counts (all channels) due to element j

or in matrix notion

$$R = AX \qquad (6)$$

which has the least-squares solution

$$X = (A^t A)^{-1} A^t R \qquad (7)$$

and the n countrates have been reduced to countrates due to each of the three radioactive elements.

Alternatively, since the error variances of the R_i are not constant, they can be 'weighted'. In this way more weight is attached to the more accurately determined R_i in the calculation of the x_j. This type of analysis assumes that the variances of the a_{ij} are negligible and that each channel contributes equally to the analysis, i.e. the information density of each channel is the same (see Crossley & Reid, 1982). In this case, given that the variance due to counting statistics, v_i, of each channel is given by (Grasty & others, 1985), viz.

$$v_i = \frac{ri}{m} + \frac{bi}{n} \qquad (8)$$

where r_i = background corrected average countrate in channel i, b_i = average background countrate in channel i, and m, n = the number of one-second samples of airborne and background data respectively, then the weighted least squares equivalent of equation (7) can be written as (Minty, 1977c)

$$X = (A^t V^{-1} A)^{-1} A^t V^{-1} R \qquad (9)$$

and the variance in the concentration vector, X, is given by (Grasty & others, 1985), viz.

$$var (X) = (A^t V^{-1})^{-1} \qquad (10)$$

APPENDIX 4

Inversion of airborne gamma-ray spectrometer data
(after Minty, 1977b)

This Appendix describes the application to airborne gamma-ray
spectrometry of an established geophysical technique for solving
the linear inverse problem. Bott (1967) originally proposed this
matrix method of determining the source distribution responsible
for a given geophysical anomaly and applied it specifically to
the determination of the source distribution causing oceanic
magnetic anomalies. The present problem is to determine the
surface distribution of radioactive material from the observed
radiometric anomaly.

Consider a continuous two-dimensional distribution of line
source emitters of various intensities. Let the line sources be
orientated perpendicular to the aircraft track, and let their
distribution be described by D(x).
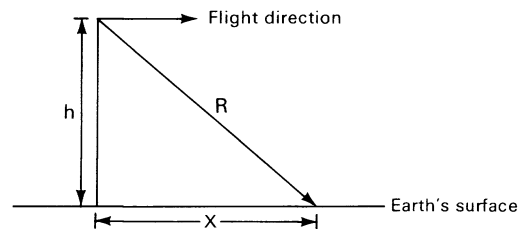
The intensity I(x,h) at (x,h) is the product of D(x) and
K(x,e,A,R,u) summed over all possible values of x, where
x = displacement along the flight direction, h = terrain
clearance, e = detector efficiency, A = area of detector,
R = distance from source point to detector, u = attenuation
coefficient of the gamma radiation in question, and K is a
function of x,e,A,R, and u, and describes the dependence of the
intensity at (x,h) on the position of a particular line source.

$$I(x,h) = \quad D(x)K(x,e,A,R,u)\ dx \qquad (1)$$

Suppose the value of the anomaly I(x,h) is known at n points.
The surface of the earth may be divided into a finite number of
surface elements (line sources of width, a, perpendicular to the

flight direction). Let there be m such elements, where n≥m; then
the integral (1) is linear (K is independent of D), and can be
replaced by a finite summation:

$$I_i = \sum_{j=1}^{m} K_{ij}D_j \quad (i=1,2.....n) \tag{2}$$

i.e., we have a set of n linear equations that can be written in
matrix notation as

$$I = KD \tag{3}$$

where K_{ij} is the intensity at the ith field point caused by the
jth surface element (i.e., line source) assuming a unit intensity
for the jth element. Equation (3) can now be solved for the
source distribution. In matrix notation,

$$\text{for } n=m, \quad D = K^{-1}I \tag{4}$$

$$\text{for } n>m, \quad D = (K^tK)^{-1}K^tI \tag{5}$$

where equation (5) is the least-squares solution for D.

TABLE 1 : ^{238}U DECAY SERIES (from Radiological Health Handbook, 1970)

Nuclide	Historical name	Half-life	Major radiation energies (MeV) and intensities†		
			α	β	γ
$^{238}_{92}$U	Uranium I	4.51×10^9 y	4.15 (25%) 4.20 (75%)	---	---
$^{234}_{90}$Th	Uranium X₁	24.1d	---	0.103 (21%) 0.193 (79%)	0.063c‡ (3.5%) 0.093c (4%)
$^{234}_{91}$Pa^m	Uranium X₂	1.17m	---	2.29 (98%)	0.765 (0.30%) 1.001 (0.60%)
$^{234}_{91}$Pa	Uranium Z	6.75h	---	0.53 (66%) 1.13 (13%)	0.100 (50%) 0.70 (24%) 0.90 (70%)
$^{234}_{92}$U	Uranium II	2.47×10^5 y	4.72 (28%) 4.77 (72%)	---	0.053 (0.2%)
$^{230}_{90}$Th	Ionium	8.0×10^4 y	4.62 (24%) 4.68 (76%)	---	0.068 (0.6%) 0.142 (0.07%)
$^{226}_{88}$Ra	Radium	1602y	4.60 (6%) 4.78 (95%)	---	0.186 (4%)
$^{222}_{86}$Rn	Emanation Radon (Rn)	3.823d	5.49 (100%)	---	0.510 (0.07%)
$^{218}_{84}$Po	Radium A	3.05m	6.00 (~100%)	0.33 (~0.019%)	---
$^{214}_{82}$Pb	Radium B	26.8m	---	0.65 (50%) 0.71 (40%) 0.98 (6%)	0.295 (19%) 0.352 (36%)
$^{218}_{85}$At	Astatine	~2s	6.65 (6%) 6.70 (94%)	? (~0.1%)	---
$^{214}_{83}$Bi	Radium C	19.7m	5.45 (0.012%) 5.51 (0.008%)	1.0 (23%) 1.51 (40%) 3.26 (19%)	0.609 (47%) 1.120 (17%) 1.764 (17%)
$^{214}_{84}$Po	Radium C'	164μs	7.69 (100%)	---	0.799 (0.014%)
$^{210}_{81}$Tl	Radium C"	1.3m	---	1.3 (25%) 1.9 (56%) 2.3 (19%)	0.296 (80%) 0.795 (100%) 1.31 (21%)
$^{210}_{82}$Pb	Radium D	21y	3.72 (.000002%)	0.016 (85%) 0.061 (15%)	0.047 (4%)
$^{210}_{83}$Bi	Radium E	5.01d	4.65 (.00007%) 4.69 (.00005%)	1.161 (~100%)	---
$^{210}_{84}$Po	Radium F	138.4d	5.305 (100%)	---	0.803 (0.0011%)
$^{206}_{81}$Tl	Radium E"	4.19m	---	1.571 (100%)	---
$^{206}_{82}$Pb	Radium G	Stable	---	---	---

Flow diagram branches:
- 99.87% | 0.13% (between Uranium X₂ and Uranium Z)
- 99.98% | 0.02% (between Radium A and Radium B/Astatine)
- 99.98% | 0.02% (between Radium C and Radium C'/Radium C")
- ~100% | .00013% (between Radium E and Radium F/Radium E")

TABLE 2 : ^{235} U DECAY SERIES (from Radiological Health Handbook, 1970)

Nuclide	Historical name	Half-life	Major radiation energies (MeV) and intensities†		
			α	β	γ
$^{235}_{92}$U	Actinouranium	7.1 ×10⁸y	4.37 (18%) 4.40 (57%) 4.58c‡ (8%)	---	0.143 (11%) 0.185 (54%) 0.204 (5%)
$^{231}_{90}$Th	Uranium Y	25.5h	---	0.140 (45%) 0.220 (15%) 0.305 (40%)	0.026 (2%) 0.084c (10%)
$^{231}_{91}$Pa	Protoactinium	3.25x10⁴y	4.95 (22%) 5.01 (24%) 5.02 (23%)	---	0.027 (6%) 0.29c (6%)
$^{227}_{89}$Ac	Actinium	21.6y	4.86c (0.18%) 4.95c (1.2%)	0.043 (~99%)	0.070 (0.08%)
$^{227}_{90}$Th	Radioactinium	18.2d	5.76 (21%) 5.98 (24%) 6.04 (23%)	---	0.050 (8%) 0.237c (15%) 0.31c (8%)
$^{223}_{87}$Fr	Actinium K	22m	5.44 (~0.005%)	1.15 (~100%)	0.050 (40%) 0.080 (13%) 0.234 (4%)
$^{223}_{88}$Ra	Actinium X	11.43d	5.61 (26%) 5.71 (54%) 5.75 (9%)	---	0.149c (10%) 0.270 (10%) 0.33c (6%)
$^{219}_{86}$Rn	Emanation Actinon (An)	4.0s	6.42 (8%) 6.55 (11%) 6.82 (81%)	---	0.272 (9%) 0.401 (5%)
$^{215}_{84}$Po	Actinium A	1.78ms	7.38 (~100%)	0.74 (~.00023%)	---
$^{211}_{82}$Pb	Actinium B	36.1m	---	0.29 (1.4%) 0.56 (9.4%) 1.39 (87.5%)	0.405 (3.4%) 0.427 (1.8%) 0.832 (3.4%)
$^{215}_{85}$At	Astatine	~0.1ms	8.01 (~100%)	---	---
$^{211}_{83}$Bi	Actinium C	2.15m	6.28 (16%) 6.62 (84%)	0.60 (0.28%)	0.351 (14%)
$^{211}_{84}$Po	Actinium C'	0.52s	7.45 (99%)	---	0.570 (0.5%) 0.90 (0.5%)
$^{207}_{81}$Tl	Actinium C"	4.79m	---	1.44 (99.8%)	0.897 (0.16%)
$^{207}_{82}$Pb	Actinium D	Stable	---	---	---

98.6%   1.4%

~100%   .00023%

0.28%   99.7%

TABLE 3 : ^{232}Th DECAY SERIES (from Radiological Health Handbook, 1970)

Nuclide	Historical name	Half-life	Major radiation energies (MeV) and intensities†		
			α	β	γ
$^{232}_{90}$Th	Thorium	1.41×10^{10}y	3.95 (24%) 4.01 (76%)	---	---
$^{228}_{88}$Ra	Mesothorium I	6.7y	---	0.055 (100%)	---
$^{228}_{89}$Ac	Mesothorium II	6.13h	---	1.18 (35%) 1.75 (12%) 2.09 (12%)	0.34c‡ (15%) 0.908 (25%) 0.96c (20%)
$^{228}_{90}$Th	Radiothorium	1.910y	5.34 (28%) 5.43 (71%)	---	0.084 (1.6%) 0.214 (0.3%)
$^{224}_{88}$Ra	Thorium X	3.64d	5.45 (6%) 5.68 (94%)	---	0.241 (3.7%)
$^{220}_{86}$Rn	Emanation Thoron (Tn)	55s	6.29 (100%)	---	0.55 (0.07%)
$^{216}_{84}$Po	Thorium A	0.15s	6.78 (100%)	---	---
$^{212}_{82}$Pb	Thorium B	10.64h	---	0.346 (81%) 0.586 (14%)	0.239 (47%) 0.300 (3.2%)
$^{212}_{83}$Bi	Thorium C	60.6m	6.05 (25%) 6.09 (10%)	1.55 (5%) 2.26 (55%)	0.040 (2%) 0.727 (7%) 1.620 (1.8%)
$^{212}_{84}$Po	Thorium C'	304ns	8.78 (100%)	---	---
$^{208}_{81}$Tl	Thorium C"	3.10m	---	1.28 (25%) 1.52 (21%) 1.80 (50%)	0.511 (23%) 0.583 (86%) 0.860 (12%) 2.614 (100%)
$^{208}_{82}$Pb	Thorium D	Stable	---	---	---

64.0%   36.0%

TABLE 4 :   MASS ATTENUATION COEFFICIENTS AND HALF-THICKNESSES FOR
            VARIOUS GAMMA-RAY ENERGIES IN AIR, WATER, AND CONCRETE
            (from Grasty, 1979)

Photon energy (MeV)	Mass-attenuation coefficient (cm^2/g)			Half thickness (a)		
	Air (b)	Water	Concrete (c)	Air (d) (m)	Water (cm)	Concrete (cm)
0.01	4.82	4.99	26.5	1.11	0.139	0.01
0.10	0.151	0.168	0.171	35.5	4.13	1.62
0.15	0.134	0.149	0.140	40.0	4.65	1.98
0.20	0.123	0.136	0.125	43.6	5.10	2.22
0.30	0.106	0.118	0.107	50.6	5.87	2.59
0.40	0.0954	0.106	0.0957	56.2	6.54	2.90
0.50	0.0868	0.0966	0.0873	61.8	7.18	3.18
0.60	0.0804	0.0894	0.0807	66.7	7.75	3.43
0.80	0.0706	0.0785	0.0708	75.9	8.83	3.92
1.0	0.0635	0.0706	0.0637	84.4	9.82	4.35
1.46	0.0526	0.0585	0.0528	102	11.8	5.25
1.5	0.0517	0.0575	0.0519	104	12.1	5.34
1.76	0.0479	0.0532	0.0482	112	13.0	5.75
2.0	0.0444	0.0493	0.0447	121	14.1	6.20
2.62	0.0391	0.0433	0.0396	137	16.0	7.00
3.0	0.0358	0.0396	0.0365	150	17.5	7.60

(a)   Thickness of material that reduces the intensity of the
      beam to half its initial value.

(b)   75.5% N, 23.2% O, 1.3% Ar by weight.

(c)   For composition of typical concrete see Hubbell &
      Berger, 1968.   Density of concrete is 2.5 g/cm^3.

(d)   For air at $0^\circ C$ and 76 cm of Hg with a density of
      0.001293 g/cm^3.

TABLE 5 : CONVENTIONAL WINDOW SETTINGS FOR THREE-CHANNEL
SPECTROMETERS

Element Analysed	Isotope used	Gamma-ray energy (MeV)	Energy window (MeV)
Potassium	^{40}K	1.46	1.37 - 1.57
Uranium	^{214}Bi	1.76	1.66 - 1.86
Thorium	^{208}Th	2.62	2.41 - 2.81